

Title

A transcallosal fiber network between left and right homotopic inferior frontal regions for supporting complex linguistic processing

Philipp Kellmeyer

Intracranial EEG and Brain Imaging Group, Department of Neurosurgery, Epilepsy Center, Medical Center – University of Freiburg, Germany

Email: philipp.kellmeyer@uniklinik-freiburg.de

Abstract

Inferior frontal regions in the left and right hemisphere support different aspects of language processing. In the classic model, left inferior frontal regions are mostly involved in processing based on phonological, syntactic and semantic features of language, whereas the right inferior frontal regions process paralinguistic aspects like affective prosody.

Using DTI-based probabilistic fiber tracking in 20 healthy volunteers, we identify a callosal fiber network connecting left and right homotopic inferior frontal regions in the context of linguistic processing of different complexity. Anatomically, we show that the interhemispheric fibers are highly aligned and distributed along a rostral to caudal gradient in the body and genu of the corpus callosum.

Functionally, our findings suggest that this transcallosal network of homotopic inferior frontal regions in the uninjured brain supports rapid integration of linguistic features of different complexity independent of emotional valence. Taking data from in-vivo neuroanatomical studies, previous DTI-based tracking studies and clinical case studies into account, we hypothesize that this role of the right inferior frontal cortex in supporting complex linguistic computations may explain patterns of right hemispheric contribution to stroke recovery as well as disorders of prosodic processing. Apart from language, inter-species differences in transcallosal connectivity and fiber density may explain differences in the ability to process complex structures between different species.

Introduction

Cumulative and converging evidence from 150 years of clinical neurology, neuroanatomy, neuropsychology and neuroimaging shows that the left and the right hemisphere support common as well as differing aspects of language processing in the brain. In this current model, the left perisylvian cortex mainly supports linguistic aspects of language processing like the analysis of phonological, syntactic or semantic features¹⁻⁴ and the right perisylvian cortex computes predominantly paralinguistic features of language like rhythm or prosody⁵⁻⁸.

Macroanatomically, the left and right inferior frontal cortex (IFC) each consists of three parts: a superior dorsal part (IFC pars opercularis and parts of ventral premotor cortex, IFC_{po/PMV}), a middle part (comprising anterior pars opercularis and posterior pars triangularis, LIFC_{po/pt}) and an anterior-inferior part (pars triangularis, IFC_{pt}). For cytoarchitecture, anatomists have found differences in volume and cell-packing density between left and right inferior frontal cortex for BA 44 and to a lesser extent for BA 45⁹. This suggests that BA 44 is more lateralized than BA 45 cytoarchitecturally.

For left inferior frontal cortex (LIFC), aggregated evidence from twenty-five years of neuroimaging studies suggests a distinct function-anatomical organization in which the anatomical tripartition reflects a functional processing gradient^{2,10-13}. In this model, the LIFC_{po/PMV} part is preferentially involved in phonological, the LIFC_{po/pt} in syntactic and the LIFG_{pt} part in semantic processing^{4,14}. Others have argued for a more supramodal view of LIFG in integrating syntactic and semantic processing^{15,16}.

The role of the homotopic right inferior frontal cortex in language processing, however, is much less clear. There is some agreement that right IFC seems to support the analysis of paralinguistic, specifically affective features of prosody^{17,18}. Prosody – the “third element” of speech as originally proposed by the Norwegian neurologist Monrad-Krohn, the founder of the modern patholinguistic study of disorders of prosody^{19,20} – is also conveyed by so-called *intrinsic* features like stress, rhythm and pitch, however, and these features are processed by right *and* left inferior frontal cortex^{2,5,21}. Thus, the dynamic interaction between left and right inferior frontal cortex seems to be a necessary condition for successful language use in real-time. The aim of our DTI-study

here is to map the white matter fiber network that provides the structural pathways to facilitate this interaction.

In terms of white matter connectivity, left and right homotopic inferior frontal cortex connect by fibers of the corpus callosum (CC). White matter fibers of the CC are among the most aligned fibers in the brain, connecting homotopic and heterotopic regions, and show high reliability in autoradiographic or MRI-based fiber tracking procedures^{22,23}.

Much of the available DTI-based studies investigating interhemispheric connectivity, however, are not grounded in or related to neurolinguistics research but look at more general patterns of CC connections often based on deterministic tractography.

Here, we use results from an fMRI language experiment in which the paradigm involved linguistic computations of different complexity for mapping the interhemispheric transcallosal fiber network between left and right inferior frontal regions with probabilistic DTI-based fiber tracking. Because the seed points for the probabilistic tractography derive from a well-controlled neurolinguistic fMRI experiment, we can relate the tracking results to specific aspect of interhemispheric callosal interaction based on linguistic complexity.

We show that highly aligned transcallosal fibers connect both left and right anterior-inferior IFC (BA45, ventral BA 44) and left and right posterior superior IFC (dorsal BA 44) to facilitate the rapid and dynamic interplay between linguistic and paralinguistic features in processing language.

Methods

fMRI paradigm

The seed points for the DTI-based tractography were derived from an fMRI study on phonological transformation by Peschke et al. (2012)²⁴. For the full description of the study and the paradigm see Peschke et al. (2012)²⁴.

Briefly, subjects in this experiment had to overtly REPEAT or TRANSFORM particular pseudo words or pseudo noun phrases (NP) in the scanner. Peschke et al. modelled the pseudo words after names of countries (e.g. “Doga” [engl. “Doga”] in analogy to

“Kuba” [engl. “Cuba”]) and the pseudo NP were modelled after monosyllabic German NP (e.g. “der Mall” [engl. e.g. “the goll”] in analogy to “der Ball” [engl. “the ball”]).

In the REPEAT condition, subjects had to just repeat the pseudo word or pseudo NP and in the TRANSFORM condition, the pseudo countries had to be transformed into the corresponding pseudo language (e.g. “Doga” -> “Doganisch” [engl. “Doga” -> “Dogan”]) and the pseudo NP into their corresponding diminutive form (e.g. “der Mall” -> “das Mällchen” [engl. e.g. “the goll” -> “the little goll”]). Linguistically, the transformation of the pseudo words entails mostly *prosodic* changes (PROSODIC), i.e. stress (“Dóga” -> “Dogánisch”), and transforming the pseudo NP requires more complex, *segmental* and *morphosyntactic* (SEGMENTAL), changes (e.g. in “der Ball” -> “das Bällchen” the segment “-all” is substituted with “-äll” and the pronoun changes from “der” to “das”).

Identification of seed points from the fMRI study

The procedure for defining the seed points was the same as described in Kellmeyer et al. (2013)¹².

For our tracking experiment only the peak coordinates from the random effects (2nd level) fMRI analysis of the contrast TRANSFORM (either PROSODIC or SEGMENTAL) minus REPETITION were used as seeds. We did not use the random effects analysis of REPETITION alone for tracking because previous experiments have already demonstrated the structural connectivity patterns in the context of repetition of pseudo words via dorsal and ventral *temporo*-frontal pathways^{25,26}.

For better demarcation in defining the seed regions we chose a different threshold ($p < 0.001$, uncorrected) for the t-maps in SPM8 than what was used in the fMRI study by Peschke et al.²⁴. Therefore, peak coordinates, cluster size and t-values partly differ from which used a threshold of $p < 0.05$, FDR-corrected for the whole brain and a cluster level of > 10 voxels. We should point out, that the sphere from which each tracking started (with a radius of 4 mm each containing 33 seed voxels) encompassed the coordinate voxels from the published version of the study by Peschke et al.²⁴ in each case. Thus, slight differences in the peak coordinates from our tracking experiment and the published version of Peschke et al. (2012)²⁴ should not be a major concern.

In the contrasts of PROSODIC(transform)-PROSODIC(repeat) and SEGMENTAL(transform)-SEGMENTAL(repeat), the peak voxel in the significant ($p < 0.001$, uncorrected) activation clusters was identified, then transformed to the native space of each subjects' DTI data and enlarged to a sphere with a radius of 4 mm each containing 33 seed voxels.

For the PROSODIC transformation condition, the peak voxel in the left parietal (left inferior parietal, LIPL) and frontal lobe (left inferior frontal gyrus, pars opercularis, LIFG_{op}) in the left hemisphere were taken as seed regions.

For the SEGMENTAL transformation condition, two parietal (anterior/posterior IPL) and two frontal peak voxels (LIFG_{op}; LIFG, pars triangularis, LIFG_{tri}) were selected in the left hemisphere. In the right hemisphere, one parietal (RIPL) and two frontal peaks (RIFG_{op}; RIFG_{tri}) were chosen as seed regions. **Figure 1** provides an overview of the fMRI results showing the seed regions.

Task in fMRI experiment	Region	Side	Cluster size (voxels)	Peak MNI coordinates			t-value*
				x	y	z	
Segmental manipulation (transform > repeat)	IFG, pars opercularis	L	1778	-48	12	27	9.38
	IFG, pars triangularis	L	1778	-45	39	9	8.26
	IFG, pars opercularis	R	613	45	12	24	5.12
	IFG, pars triangularis	R	613	45	36	12	6.01

Table 1 lists the respective coordinate clusters in MNI-space.

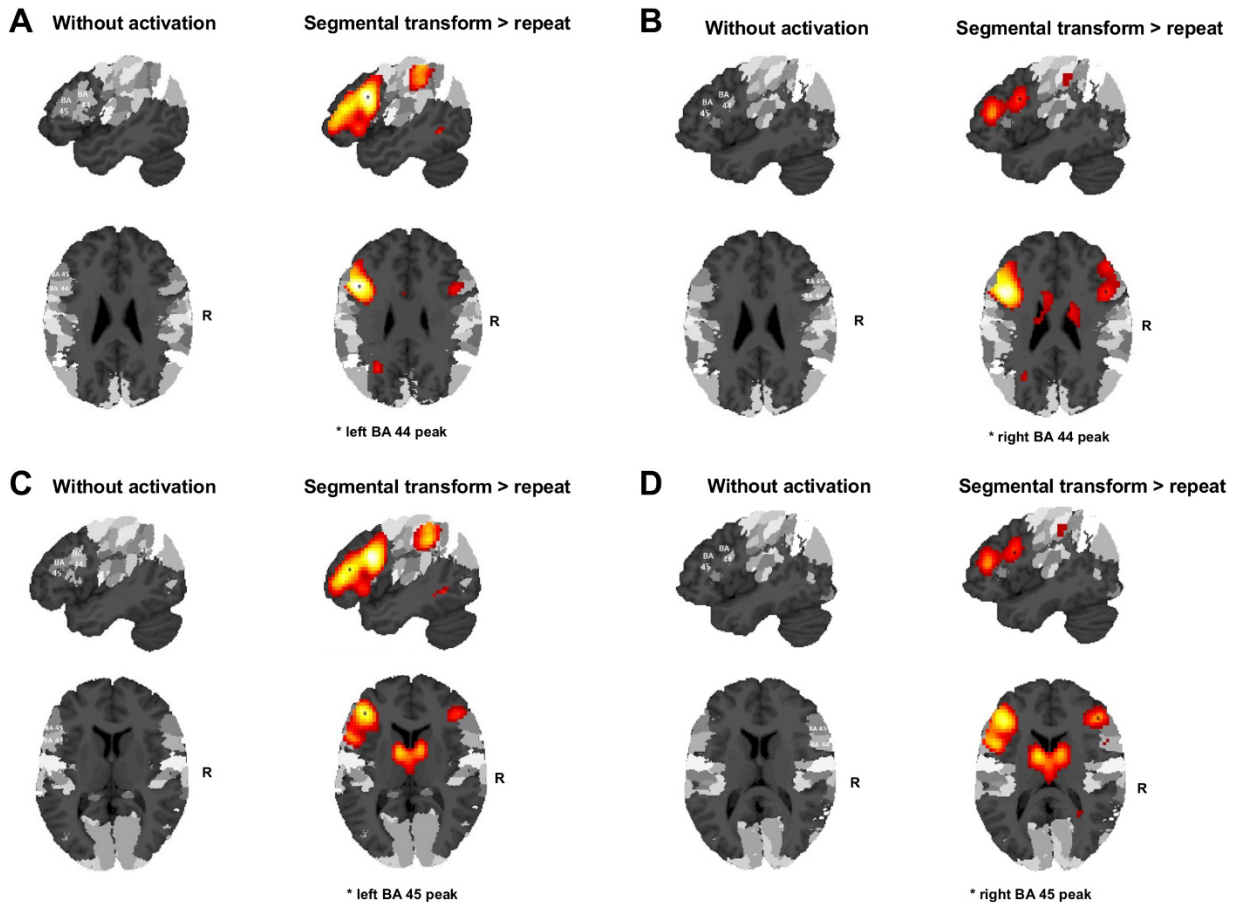


Figure 1 Peak activation clusters in left and right inferior frontal cortex from the fMRI experiment by Peschke et al. (2012) that were used as seed points for the interhemispheric probabilistic DTI-based fiber tracking in our group of volunteers. Activation clusters are displayed at $p < 0.05$, FDR-corrected and superimposed on the cytoarchitectonic probability atlas by Eickhoff et al. (2005)²⁷ in SPM8.

Task in fMRI experiment	Region	Side	Cluster size (voxels)	Peak MNI coordinates			
				x	y	z	t-value*
Segmental manipulation (transform > repeat)	IFG, pars opercularis	L	1778	-48	12	27	9.38
	IFG, pars triangularis	L	1778	-45	39	9	8.26

IFG, pars opercularis	R	613	45	12	24	5.12
IFG, pars triangularis	R	613	45	36	12	6.01

Table 1 Peak activation clusters from the fMRI study by Peschke et al. (2012). Activation clusters
* uncorrected at $p < 0.001$

Participants and group matching

The participants and the procedure for matching participants from the DTI group to the fMRI group from Peschke et al. (2012)²⁴ were the same as described in Kellmeyer et al. (2013)¹².

In the study by Peschke et al. (2012)²⁴, the researchers did not obtain DTI sequences from the participants in the fMRI study. For the DTI study presented here, we therefore matched twenty subjects in age, gender and handedness to the fMRI group. As in the fMRI study, all subjects were also native German speakers without any history of serious medical, neurological or psychiatric illness. The DTI study was approved by the Ethics Committee of the University Medical Center in Freiburg and all subjects gave written informed consent. The mean age in the DTI group was 24 years, the age range 20-38 years and 8 females and 12 males participated. Hand preference was tested with the 10-item version of the Edinburgh Handedness Inventory²⁸, subjects were identified as having predominantly right hand preference with an average laterality quotient of 0.8 (range 0.55-1.0). This group did not differ significantly from the fMRI group from Peschke et al. (2012)²⁴ in terms of age, gender or handedness.

The matching of the groups should account for the majority of gross anatomical differences between two groups of healthy individuals (see also Suchan et al. 2013 and Kellmeyer et al. 2013^{12,29}). Furthermore, all subjects' anatomical scans (T1) were checked for gross anatomical anomalies (if necessary with expertise from a qualified neuroradiologist).

Image acquisition

We acquired high angular resolution diffusion imaging (HARDI) data with a 3 Tesla *Siemens MAGNETOM Trio TIM* scanner using a diffusion-sensitive spin-echo echo planar imaging sequence with suppression of the cerebrospinal fluid signal. In total, we

acquired 70 scans (with 69 slices) with 61 diffusion-encoding gradient directions (b-factor = 1000 s/mm) and 9 scans without diffusion weighting (b-factor = 0). The sequence parameters were: voxel size = $2 \times 2 \times 2$ mm³, matrix size = 104×104 pixel², TR = 11.8 s, TE = 96 ms, TI = 2.3 s. We corrected all scans for motion and distortion artifacts based on a reference measurement during reconstruction³⁰. Finally, we obtained a high-resolution T1 anatomical scan (160 slices, voxel size = $1 \times 1 \times 1$ mm³, matrix= 240×240 pixel², TR=2.2 s, TE=2.6ms) for spatial processing of the DTI data.

Probabilistic tracking

We analyzed the DTI data by using the method of pathway extraction introduced by Kreher et al. (2008) which is part of the Matlab-based “DTI&Fiber toolbox”³¹. This toolbox is available online for download (http://www.uniklinik-freiburg.de/mr/live/arbeitsgruppen/diffusion_en.html). Previously, this method has been used to identify white matter connections involved in language processing^{12,25,26}, attention³² and motor cognition^{33,34}.

For this procedure, we first computed the effective self-diffusion tensor (sDT) from the HARDI dataset³⁵, which was corrected for movement and distortion artifacts.

Then, we performed a Monte Carlo simulation of “random walks” to calculate the probabilistic maps for each seed region separately. This procedure is similar to the Probabilistic Index of Connectivity (PICO) method³⁶. In extension to the PICO method, our probabilistic MCRW experiment preserves the information about the main traversing directions of the propagated fiber trajectories for each voxel. We then used this information for combining the probability maps. We extracted the orientation density function empirically from the effective diffusion tensor. The number of propagated trajectories was set to 10 and maximal fiber length was set to 150 voxels in accordance with our experience from the previous tracking studies mentioned above. We restricted the tracking area in each individual by a white matter mask to avoid tracking across anatomical borders. This mask included a small rim of grey matter to ensure that the cortical seed regions had indeed contact with the underlying white matter tracts.

To compute region-to-region anatomical connectivity between two seed spheres, we used a pairwise combination of two probability maps of interest³¹. Computationally, this

combination is a multiplication, which takes the main traversing trajectory of the random walk into account. Random walks starting from seed regions may face in either *opposing* directions (connecting fibers) or merge and face in the *same* direction (merging fibers). In a pathway connecting two seed regions, the proportion of connecting fibers should exceed the proportion of merging fibers. Using this directional information during the multiplication, merging fibers are suppressed and connecting fibers are preserved by the tracking algorithm³¹. This procedure allows for extracting the most probable connecting pathway between two seed spheres without relying on a *priori* knowledge about the putative course of the white matter fibers. The resulting values represent a voxel-wise estimation of the probability that a particular voxel is part of the connecting fiber bundle of interest (represented by a "probability index forming part of the bundle of interest" [PIBI]). In order to extract the most probable fiber tracts connecting left and right inferior frontal regions, all left inferior frontal maps were combined permutatively with all right inferior frontal maps based on the respective linguistic context (prosodic or segmental manipulation).

Post-processing of the individual probability maps

We scaled the individual probability maps to a range between 0 and 1. Then we spatially normalized the maps into standard Montreal Neurological Institute (MNI) space and subsequently smoothed them with an isotropic Gaussian kernel (3 mm) using SPM8. We computed *group maps* for each connection between seed regions by averaging the combined probability maps from all subjects. This resulted in one *mean group map* for each connection. Thus, any voxel in these group maps represents the arithmetic mean of the PIBI across subjects. To remove random artifacts, only voxels with PIBI values of >0.0145 were displayed, which excludes 95% of the voxels with PIBI $>10^{-6}$. This cutoff value was empirically derived from the distribution observed in a large collection of preprocessed combined probability maps²⁵. At the group level ($n=20$) we used a non-parametric statistic because PIBI values are not normally distributed²⁶.

Visualization

We visualized the resulting combined probability maps with the Matlab-based “DTI&Fiber Toolbox”, *MRicron* (<http://www.sph.sc.edu/comd/rorden/mricron/>) for 2D sections and a visualization program based on IBM’s *OpenDX* (<http://www.research.ibm.com/dx/>) for 3D images.

Results

The transcallosal fiber pathways between the left and right IFG show a homotopic pattern of connectivity and the fiber systems are clearly segregated and aligned in a rostral (left↔right IFC, pars triangularis, BA45 and ventral BA44) to caudal (left↔right pars opercularis, BA 44) gradient in the body and genu of the corpus callosum.

Figure 2 shows the transcallosal fiber pathways from the tracking experiment connecting left and right frontal regions. The interhemispheric frontal pathways are oriented closely together, with the connection between left BA 44 and its right hemispheric homotopic area running through the body of the CC and the connections between left BA 45 and its right homotopic area crossing more rostral in the genu.

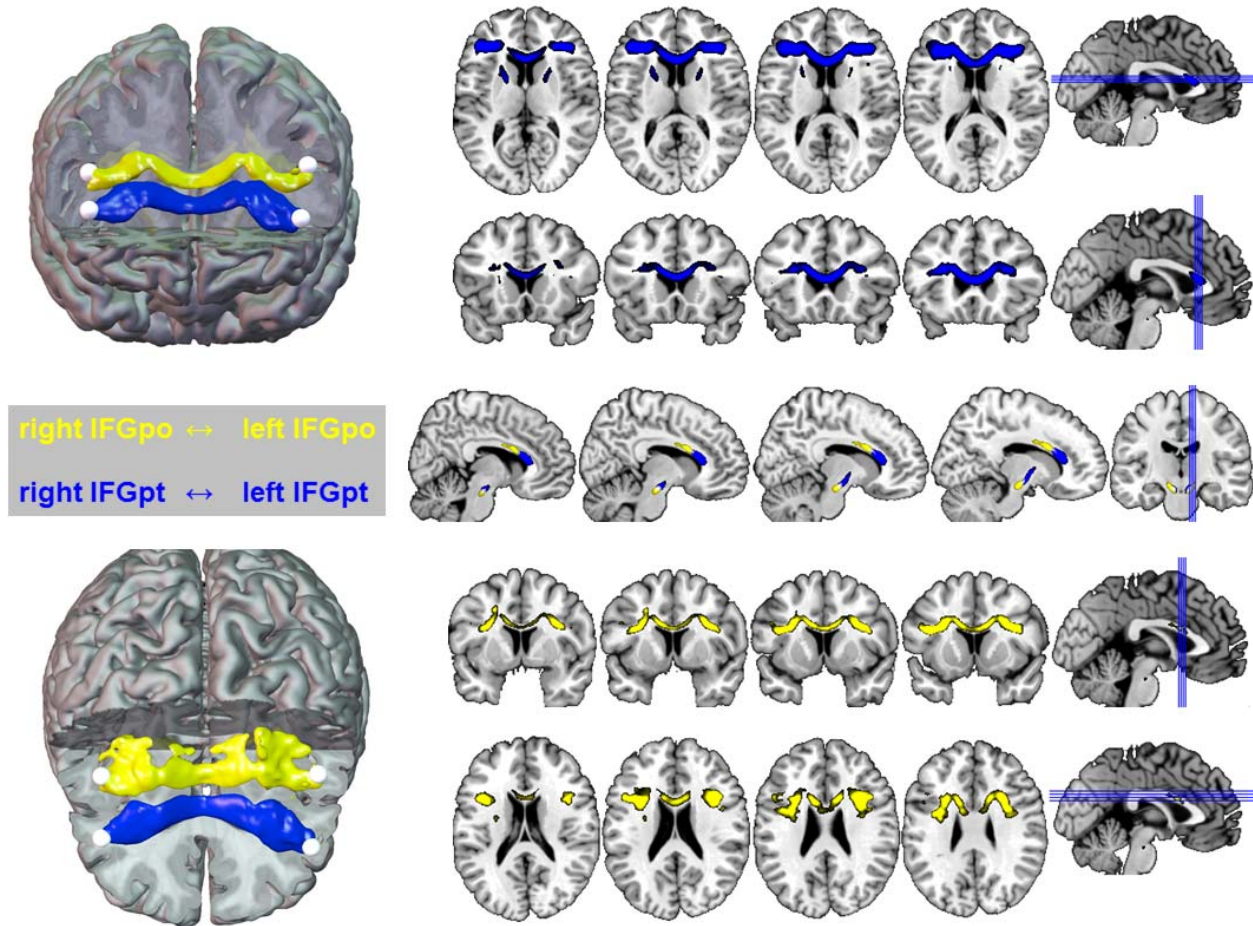


Figure 2 Results from the probabilistic fiber tracking from left to right inferior frontal gyrus (pars opercularis, IFGpo, BA 44, in yellow) and left to right inferior frontal gyrus (pars triangularis, IFGpt, B45 and ventral BA44, in blue).

Discussion

The highly aligned transcallosal white matter pathways described here demonstrate a direct interhemispheric pathway for interaction between left and right homotopic inferior frontal cortex for language processing. The results are in agreement with previous anatomical *ex vivo* studies in humans on the topography of interhemispheric callosal fibers^{37,38}, as well as *in vivo* DTI-based parcellation studies^{22,39–43}. The results also show a close cross-species correspondence to homotopic patterns of interhemispheric fibers in non-human primates^{44–46}. Next, we first discuss the putative functional role of this transcallosal pathway connecting homotopic left and inferior frontal cortex for language processing in the healthy brain. Then, we analyze the potential role of this

interhemispheric network for language reorganization and close with some remarks on comparative inter-species anatomy of the CC and its possible role for cognition.

Function of interhemispheric inferior frontal connections for language processing

In terms of functional significance, this transcallosal route may generally facilitate rapid neural processing for a variety of cognitive functions that involve homotopic inferior frontal regions in both hemispheres. In our own area of expertise - language function in the healthy and injured brain - it has long been recognized, that right and left inferior frontal cortex contribute substantially to paralinguistic aspects of language processing like prosody⁴⁷⁻⁴⁹ and/or speech rhythm⁵⁰⁻⁵². More specifically, *intrinsic* (also called linguistic) features of prosody like stress, rhythm and pitch seem to come about through damage to *left* inferior frontal regions, whereas lesions to *right* inferior cortex often results in impaired processing of *extrinsic* features of speech like affective prosody – the tonal variation conveying emotions^{8,17,18,49,53}.

Relating this model of prosodic processing to the functional and structural interhemispheric inferior frontal network identified here, we propose the following interpretation: The transformation of the pseudo country into the respective pseudo language entails a shift of stress (“Dóga” -> “Dogánisch”) which is a clear feature of linguistic prosody. This PROSODIC transformation condition (not shown in Figure 1, see Peschke et al. 2012) resulted in purely left fronto-parietal activation, which is consistent with the putative role of LIFG in intrinsic / linguistic prosodic features of language in the models mentioned above. In the SEGMENTAL transformation task of the pseudo noun phrases (“Der Mall” -> “Das Mällchen”), more complex linguistic operations occur like morphosyntactic changes and a change of the pronoun. At the level of extrinsic / affective prosody, the features most often associated with the right IFC in the classic models, it would be difficult to construe different emotional valences of the pseudo- stimuli in the prosodic vs. the segmental transformation condition.

Therefore, we interpret the involvement of right inferior frontal areas to reflect the greater *linguistic complexity* of the stimuli in the SEGMENTAL transformation condition. This is in accordance with previous fMRI studies and meta-analyses that have shown a right inferior frontal involvement in the context of complex linguistic processing

independent of emotional content^{2,13,21}.

One important open question, which we cannot answer in the context of the study here is, whether the functional effect of this interhemispheric callosal transfer is predominantly excitatory or inhibitory^{54–56}.

With respect to the functional importance of the callosal fibers, the clinical literature too allows only for very limited and preliminary conclusions. Only very few clinical reports, let alone systematic studies, on the consequences for language processing of direct damage to callosal fibers connecting left and right inferior frontal cortex are available. Mostly, callosal dysfunction in relation to language was investigated in the context of congenital callosal disorders like agenesis or dysgenesis of the CC^{57–61}. These studies have identified deficits in phonological and syntactic processing in relation to congenital CC dysfunction^{59,61–63}. Direct non-developmental callosal damage is a rare clinical event, mostly as a result of ischemic stroke or cerebral vasculitis⁶⁴. With respect to subsequent language dysfunction, we found only one report that describes a patient with a hemorrhagic lesion of the anterior part of the corpus callosum without damage to cortical projection areas⁶⁵. The patient initially showed a complete aprosody, that is a lack of tonal variation and reduced speed of speech, which recovered substantially throughout the follow-up period of one year.

From this body of clinical studies, it is difficult to infer whether callosal fibers predominantly have an inhibitory or excitatory role in the transfer of linguistic computations in the brain. Next, we therefore highlight evidence from neuroimaging and non-invasive neurostimulation studies and research on language reorganization to shed light on the putative role of callosal fibers.

The role of inferior frontal callosal connections for language reorganization

fMRI studies on the dynamics of language reorganization have shown increased activity of right-hemispheric inferior frontal region following left hemispheric stroke in homologous inferior frontal cortex with post-stroke aphasia which has been interpreted as a sign of adaptive plasticity^{66,67}. Importantly, the early up-regulation in the right hemisphere occurs in homotopic regions to the left hemispheric injured region which supports an important role of callosal fibers connecting homotopic regions⁶⁸. Further

evidence corroborating the concept of right hemispheric involvement in aphasia recovery comes from research applying rTMS-based continuous theta burst stimulation (cTBS) over the left inferior frontal gyrus⁶⁹. In this study, the virtual lesion of left inferior frontal cortex with cTBS resulted in up-regulation of the homotopic right inferior frontal cortex in reaction to the perturbation⁷⁰. The integrity of the interhemispheric white matter fiber network may therefore be critical to allow for adaptive recovery based on cross-hemispheric transfer. These studies on actual aphasia recovery and virtual lesion modelling support the concept of interhemispheric *inhibition* as the main role of homotopic inferior frontal callosal fibers^{54,71}. This concept opens avenues for further exploring new concepts for stroke recovery with non-invasive and invasive (epidural) neurostimulation as an emerging therapeutic approach⁷²⁻⁷⁵.

To summarize, we interpret the homotopic interhemispheric inferior frontal white matter pathways, which we found here, as follows: Co-activation of homotopic inferior frontal regions – connected via homotopic callosal fibers - during language processing in the uninjured brain most likely supports integration of different levels of linguistic complexity. In this model, left inferior frontal regions would be sufficient to support linguistic transformations based on basic prosodic changes (like a shift of stress), whereas more complex linguistic operations, like segmental changes, additionally tap right inferior frontal regions for complementary computations. However, as real-time language comprehension and production requires fast information transfer for integration, it may be that this model of cooperative hierarchical processing of left and right IFC prefers homotopic regions. Processing of paralinguistic features like emotional prosody, which is less time-sensitive than computing linguistic features, in turn, may not depend upon strict homotopic connections. This model accounts for the hemispheric adaptive patterns in stroke recovery discussed above, as well as the neurotypology of disorders of prosodic perception and production as a result of right hemispheric inferior frontal injury^{7,48,49}.

Finally, as this study is an in-vivo anatomical study based on DTI, we want to highlight briefly some interesting inter-species features of the anatomy and function of the CC.

Some remarks on interspecies anatomy and function of the corpus callosum

From an evolutionary and mammalian inter-species perspective, the CC is a highly conserved macroanatomic structure, indicating that it is important for supporting a variety of interhemispheric computations, independent of but in humans including language processing^{76–78}. A MRI tractography study in chimpanzees, the closest species related to humans which has been studied with DTI to date, shows a very similar topical pattern of interhemispheric connections and fiber alignment in the CC as human tractography studies and our results here⁴⁶. If we move further away in the eutherian clade of our evolutionary ancestry, however, fine differences in CC microstructure and connectivity emerge. In the largest cross-species study to date, Olivares et al. (2001)⁷⁸ demonstrated that the proportional numeric composition of fibers of the CC is preserved across six different species (the rat, the rabbit, the cat, the dog, the horse and the cow). Whereas the number of callosal fibers does not scale with increased brain size, the fiber diameter (and hence conduction velocity) does. This indicates that the type of fiber and quite likely also the pattern of connectivity might determine interhemispheric information transfer capabilities and that callosal transmission time may not be constant across species. These fine differences in interhemispheric network architecture and conduction properties, in turn, may relate to differences in the cognitive abilities of different mammalian species through timing constraints⁷⁹. For humans this structurally and functionally honed interplay and division of labor between the left and right hemisphere may indeed be the prerequisite for complex cognition and hence “the human condition” (Gazzaniga, 2000)⁸⁰.

With respect to interindividual differences in transcallosal information transfer capacity in humans, our increasing imaging resolution and increasing field strengths may be useful to explore the relationship between DTI metrics and psychometric parameters of interhemispheric information transfer in different cognitive domains in the future.

Bibliography

1. Price, C. J. A review and synthesis of the first 20 years of PET and fMRI studies of heard speech, spoken language and reading. *NeuroImage* **62**, 816–847 (2012).
2. Vigneau, M. *et al.* Meta-analyzing left hemisphere language areas: Phonology, semantics, and sentence processing. *NeuroImage* **30**, 1414–1432 (2006).

3. Hillis, A. E. Aphasia Progress in the last quarter of a century. *Neurology* **69**, 200–213 (2007).
4. Shalom, D. B. & Poeppel, D. Functional Anatomic Models of Language: Assembling the Pieces. *The Neuroscientist* **14**, 119–127 (2008).
5. Frühholz, S., Gschwind, M. & Grandjean, D. Bilateral dorsal and ventral fiber pathways for the processing of affective prosody identified by probabilistic fiber tracking. *NeuroImage* **109**, 27–34 (2015).
6. Sammler, D., Grosbras, M.-H., Anwander, A., Bestelmeyer, P. E. G. & Belin, P. Dorsal and Ventral Pathways for Prosody. *Curr. Biol.* **25**, 3079–3085 (2015).
7. Blonder, L. X., Bowers, D. & Heilman, K. M. The Role of the Right Hemisphere in Emotional Communication. *Brain* **114**, 1115–1127 (1991).
8. Ross, E. D., Thompson, R. D. & Yenkosky, J. Lateralization of Affective Prosody in Brain and the Callosal Integration of Hemispheric Language Functions. *Brain Lang.* **56**, 27–54 (1997).
9. Amunts, K. *et al.* Broca's region revisited: Cytoarchitecture and intersubject variability. *J. Comp. Neurol.* **412**, 319–341 (1999).
10. Bookheimer, S. FUNCTIONAL MRI OF LANGUAGE: New Approaches to Understanding the Cortical Organization of Semantic Processing. *Annu. Rev. Neurosci.* **25**, 151–188 (2002).
11. Poeppel, D., Emmorey, K., Hickok, G. & Pylkkänen, L. Towards a new neurobiology of language. *J. Neurosci. Off. J. Soc. Neurosci.* **32**, 14125–14131 (2012).
12. Kellmeyer, P. *et al.* Fronto-parietal dorsal and ventral pathways in the context of different linguistic manipulations. *Brain Lang.* **127**, 241–250 (2013).
13. Price, C. J. The anatomy of language: a review of 100 fMRI studies published in 2009. *Ann. N. Y. Acad. Sci.* **1191**, 62–88 (2010).
14. Dapretto, M. & Bookheimer, S. Y. Form and Content: Dissociating Syntax and Semantics in Sentence Comprehension. *Neuron* **24**, 427–432 (1999).
15. Bornkessel-Schlesewsky, I., Schlesewsky, M. & Cramon, D. Y. von. Word order and Broca's region: Evidence for a supra-syntactic perspective. *Brain Lang.* **111**, 125–139 (2009).

16. Bornkessel-Schlesewsky, I. & Schlesewsky, M. Reconciling time, space and function: A new dorsal–ventral stream model of sentence comprehension. *Brain Lang.* **125**, 60–76 (2013).
17. Ross, E. D. Nonverbal aspects of language. *Neurol. Clin.* **11**, 9–23 (1993).
18. Heilman, K. M., Bowers, D., Speedie, L. & Coslett, H. B. Comprehension of affective and nonaffective prosody. *Neurology* **34**, 917–921 (1984).
19. Monrad-Krohn, G. H. The Prosodic Quality of Speech and Its Disorders: (a Brief Survey from a Neurologist’s Point of View). *Acta Psychiatr. Scand.* **22**, 255–269 (1947).
20. Monrad-Krohn, G. H. The Third Element of Speech: Prosody in the Neuro-Psychiatric Clinic. *Br. J. Psychiatry* **103**, 326–331 (1957).
21. Vigneau, M. *et al.* What is right-hemisphere contribution to phonological, lexico-semantic, and sentence processing?: Insights from a meta-analysis. *NeuroImage* **54**, 577–593 (2011).
22. Park, H.-J. *et al.* Corpus callosal connection mapping using cortical gray matter parcellation and DT-MRI. *Hum. Brain Mapp.* **29**, 503–516 (2008).
23. Kim, E. Y., Park, H.-J., Kim, D.-H., Lee, S.-K. & Kim, J. Measuring Fractional Anisotropy of the Corpus Callosum Using Diffusion Tensor Imaging: Mid-Sagittal versus Axial Imaging Planes. *Korean J. Radiol.* **9**, 391–395 (2008).
24. Peschke, C., Ziegler, W., Eisenberger, J. & Baumgaertner, A. Phonological manipulation between speech perception and production activates a parieto-frontal circuit. *NeuroImage* **59**, 788–799 (2012).
25. Saur, D. *et al.* Ventral and dorsal pathways for language. *Proc. Natl. Acad. Sci. U. S. A.* **105**, 18035–18040 (2008).
26. Saur, D. *et al.* Combining functional and anatomical connectivity reveals brain networks for auditory language comprehension. *NeuroImage* **49**, 3187–3197 (2010).

27. Eickhoff, S. B. *et al.* A new SPM toolbox for combining probabilistic cytoarchitectonic maps and functional imaging data. *NeuroImage* **25**, 1325–1335 (2005).
28. Oldfield, R. C. The assessment and analysis of handedness: the Edinburgh inventory. *Neuropsychologia* **9**, 97–113 (1971).
29. Suchan, J. *et al.* Fiber pathways connecting cortical areas relevant for spatial orienting and exploration. *Hum. Brain Mapp.* **35**, 1031–1043 (2014).
30. Zaitsev, M., Hennig, J. & Speck, O. Point spread function mapping with parallel imaging techniques and high acceleration factors: fast, robust, and flexible method for echo-planar imaging distortion correction. *Magn. Reson. Med.* **52**, 1156–1166 (2004).
31. Kreher, B. W. *et al.* Connecting and merging fibres: Pathway extraction by combining probability maps. *NeuroImage* **43**, 81–89 (2008).
32. Umarova, R. M. *et al.* Structural Connectivity for Visuospatial Attention: Significance of Ventral Pathways. *Cereb. Cortex* **20**, 121–129 (2010).
33. Vry, M.-S. *et al.* Ventral and dorsal fiber systems for imagined and executed movement. *Exp. Brain Res.* **219**, 203–216 (2012).
34. Hamzei, F. *et al.* The Dual-Loop Model and the Human Mirror Neuron System: an Exploratory Combined fMRI and DTI Study of the Inferior Frontal Gyrus. *Cereb. Cortex* bhv066 (2015). doi:10.1093/cercor/bhv066
35. Basser, P. J., Mattiello, J. & LeBihan, D. Estimation of the effective self-diffusion tensor from the NMR spin echo. *J. Magn. Reson. B* **103**, 247–254 (1994).
36. Parker, G. J. M., Haroon, H. A. & Wheeler-Kingshott, C. A. M. A framework for a streamline-based probabilistic index of connectivity (PICO) using a structural interpretation of MRI diffusion measurements. *J. Magn. Reson. Imaging JMRI* **18**, 242–254 (2003).
37. Hewitt, W. The development of the human corpus callosum. *J. Anat.* **96**, 355–358 (1962).

38. Tomasch, J. Size, distribution, and number of fibres in the human corpus callosum. *Anat. Rec.* **119**, 119–135 (1954).
39. Huang, H. *et al.* DTI tractography based parcellation of white matter: Application to the mid-sagittal morphology of corpus callosum. *NeuroImage* **26**, 195–205 (2005).
40. Hofer, S. & Frahm, J. Topography of the human corpus callosum revisited—Comprehensive fiber tractography using diffusion tensor magnetic resonance imaging. *NeuroImage* **32**, 989–994 (2006).
41. Fabri, M., Pierpaoli, C., Barbaresi, P. & Polonara, G. Functional topography of the corpus callosum investigated by DTI and fMRI. *World J. Radiol.* **6**, 895–906 (2014).
42. Teipel, S. J. *et al.* Regional networks underlying interhemispheric connectivity: An EEG and DTI study in healthy ageing and amnesic mild cognitive impairment. *Hum. Brain Mapp.* **30**, 2098–2119 (2009).
43. Chao, Y.-P. *et al.* Probabilistic topography of human corpus callosum using cytoarchitectural parcellation and high angular resolution diffusion imaging tractography. *Hum. Brain Mapp.* **30**, 3172–3187 (2009).
44. Pandya, D. N., Karol, E. A. & Heilbronn, D. The topographical distribution of interhemispheric projections in the corpus callosum of the rhesus monkey. *Brain Res.* **32**, 31–43 (1971).
45. Makris, N. *et al.* Frontal connections and cognitive changes in normal aging rhesus monkeys: a DTI study. *Neurobiol. Aging* **28**, 1556–1567 (2007).
46. Phillips, K. A. & Hopkins, W. D. Topography of the Chimpanzee Corpus Callosum. *PLoS ONE* **7**, (2012).
47. George MS, Parekh PI, Rosinsky N & et al. UNderstanding emotional prosody activates right hemisphere regions. *Arch. Neurol.* **53**, 665–670 (1996).

48. Hoekert, M., Vingerhoets, G. & Aleman, A. Results of a pilot study on the involvement of bilateral inferior frontal gyri in emotional prosody perception: an rTMS study. *BMC Neurosci.* **11**, 93 (2010).
49. Belyk, M. & Brown, S. Perception of affective and linguistic prosody: an ALE meta-analysis of neuroimaging studies. *Soc. Cogn. Affect. Neurosci.* **9**, 1395–1403 (2014).
50. Geiser, E., Zaehle, T., Jancke, L. & Meyer, M. The Neural Correlate of Speech Rhythm as Evidenced by Metrical Speech Processing. *J. Cogn. Neurosci.* **20**, 541–552 (2007).
51. Jungblut, M., Huber, W., Pustelniak, M. & Schnitker, R. The impact of rhythm complexity on brain activation during simple singing: An event-related fMRI study. *Restor. Neurol. Neurosci.* **30**, (2012).
52. Riecker, A., Wildgruber, D., Dogil, G., Grodd, W. & Ackermann, H. Hemispheric Lateralization Effects of Rhythm Implementation during Syllable Repetitions: An fMRI Study. *NeuroImage* **16**, 169–176 (2002).
53. Speedie LJ, Coslett H & Heilman KM. REpetition of affective prosody in mixed transcortical aphasia. *Arch. Neurol.* **41**, 268–270 (1984).
54. Bloom, J. S. & Hynd, G. W. The Role of the Corpus Callosum in Interhemispheric Transfer of Information: Excitation or Inhibition? *Neuropsychol. Rev.* **15**, 59–71 (2005).
55. Reggia, J. A., Goodall, S. M., Shkuro, Y. & Glezer, M. The callosal dilemma: Explaining diaschisis in the context of hemispheric rivalry via a neural network model. *Neurol. Res.* **23**, 465–471 (2001).
56. van der Knaap, L. J. & van der Ham, I. J. M. How does the corpus callosum mediate interhemispheric transfer? A review. *Behav. Brain Res.* **223**, 211–221 (2011).
57. Brown, W. S., Symington, M., VanLancker-Sidtis, D., Dietrich, R. & Paul, L. K. Paralinguistic processing in children with callosal agenesis: Emergence of neurolinguistic deficits. *Brain Lang.* **93**, 135–139 (2005).

58. Genç, E., Ocklenburg, S., Singer, W. & Güntürkün, O. Abnormal interhemispheric motor interactions in patients with callosal agenesis. *Behav. Brain Res.* **293**, 1–9 (2015).
59. Jeeves, M. A. & Temple, C. M. A further study of language function in callosal agenesis. *Brain Lang.* **32**, 325–335 (1987).
60. Paul, L. K., Van Lancker-Sidtis, D., Schieffer, B., Dietrich, R. & Brown, W. S. Communicative deficits in agenesis of the corpus callosum: Nonliteral language and affective prosody. *Brain Lang.* **85**, 313–324 (2003).
61. Sanders, R. J. Sentence comprehension following agenesis of the corpus callosum. *Brain Lang.* **37**, 59–72 (1989).
62. Paul, L. K., Van Lancker-Sidtis, D., Schieffer, B., Dietrich, R. & Brown, W. S. Communicative deficits in agenesis of the corpus callosum: Nonliteral language and affective prosody. *Brain Lang.* **85**, 313–324 (2003).
63. Temple, C. M., Jeeves, M. A. & Vilarroya, O. Ten pen men: rhyming skills in two children with callosal agenesis. *Brain Lang.* **37**, 548–564 (1989).
64. Mahale, R. *et al.* Diffuse corpus callosum infarction — Rare vascular entity with differing etiology. *J. Neurol. Sci.* **360**, 45–48 (2016).
65. Klouda, G. V., Robin, D. A., Graff-Radford, N. R. & Cooper, W. E. The role of callosal connections in speech prosody. *Brain Lang.* **35**, 154–171 (1988).
66. Saur, D. *et al.* Dynamics of language reorganization after stroke. *Brain* **129**, 1371–1384 (2006).
67. Winhuisen, L. *et al.* The Right Inferior Frontal Gyrus and Poststroke Aphasia A Follow-Up Investigation. *Stroke* **38**, 1286–1292 (2007).
68. Staudt, M. *et al.* Right-Hemispheric Organization of Language Following Early Left-Sided Brain Lesions: Functional MRI Topography. *NeuroImage* **16**, 954–967 (2002).

69. Hartwigsen, G. *et al.* Perturbation of the left inferior frontal gyrus triggers adaptive plasticity in the right homologous area during speech production. *Proc. Natl. Acad. Sci.* **110**, 16402–16407 (2013).
70. Hartwigsen, G. The neurophysiology of language: Insights from non-invasive brain stimulation in the healthy human brain. *Brain Lang.* **148**, 81–94 (2015).
71. Kano, T., Kobayashi, M., Ohira, T. & Yoshida, K. Speech-induced modulation of interhemispheric inhibition. *Neurosci. Lett.* **531**, 86–90 (2012).
72. Ota, B., Olma, M. C., Flöel, A. & Wellwood, I. Inhibitory non-invasive brain stimulation to homologous language regions as an adjunct to speech and language therapy in post-stroke aphasia: a meta-analysis. *Front. Hum. Neurosci.* **9**, (2015).
73. Hamilton, R. H., Chrysikou, E. G. & Coslett, B. Mechanisms of Aphasia Recovery After Stroke and the Role of Noninvasive Brain Stimulation. *Brain Lang.* **118**, 40–50 (2011).
74. Balossier, A., Etard, O., Descat, C., Vivien, D. & Emery, E. Epidural Cortical Stimulation as a Treatment for Poststroke Aphasia A Systematic Review of the Literature and Underlying Neurophysiological Mechanisms. *Neurorehabil. Neural Repair* 1545968315606989 (2015). doi:10.1177/1545968315606989
75. Cherney, L. R. Epidural Cortical Stimulation as Adjunctive Treatment for Nonfluent Aphasia Phase 1 Clinical Trial Follow-up Findings. *Neurorehabil. Neural Repair* 1545968315622574 (2015). doi:10.1177/1545968315622574
76. Aboitiz, F. & Montiel, J. One hundred million years of interhemispheric communication: the history of the corpus callosum. *Braz. J. Med. Biol. Res.* **36**, 409–420 (2003).
77. Olivares, R., Michalland, S. & Aboitiz, F. Cross-Species and Intraspecies Morphometric Analysis of the Corpus Callosum. *Brain. Behav. Evol.* **55**, 37–43 (2000).
78. Olivares, R., Montiel, J. & Aboitiz, F. Species Differences and Similarities in the Fine Structure of the Mammalian Corpus callosum. *Brain. Behav. Evol.* **57**, 98–105 (2001).

79. Aboitiz, F., López, J. & Montiel, J. Long distance communication in the human brain: timing constraints for inter-hemispheric synchrony and the origin of brain lateralization. *Biol. Res.* **36**, 89–99 (2003).
80. Gazzaniga, M. S. Cerebral specialization and interhemispheric communication. *Brain* **123**, 1293–1326 (2000).